DOI: 10.1002/chem.200500970

Frontal Polymerization Synthesis of Starch-Grafted Hydrogels: Effect of Temperature and Tube Size on Propagating Front and Properties of Hydrogels

Qing-Zhi Yan, Wen-Feng Zhang, Guo-Dong Lu, Xin-Tai Su, and Chang-Chun Ge*[a]

Abstract: The frontal polymerization process was used to produce superabsorbent hydrogels based on acrylic acid monomers grafted onto starch. Using a simple test tube which was nonadiabatic and permitted contact with air, the effects of initial temperature and tube size on the propagating front of grafting copolymerization and the properties of hydrogels were explored. The unrestricted access of the reaction mixture to oxygen delayed the formation of self-propagating polymerization front. The ignition time was markedly lengthened with the increasing of tube size attributed to the formation of large amounts of peroxy radicals. The front velocity dependence on initial temperature could be fit to an Arrhenius function with the average apparent activation energy of 24 kJ mol^{-1}, and on tube size to a function of higher order. The increase of the initial temperature increased the front temperature, which lead to more soluble oligomers and higher degree of crosslinking. The interplay of two opposite effects of oligomer and crosslinking determined the sol and gel content. An increase in tube size had two effects on the propagating front. One was to reduce heat loss. The other effect was to increase the number of escaping gas bubbles. The combined action of the two effects resulted in a maximum value of front temperature, an increase in sol content and a reduction in gel content with tube size. The highest swelling capacity of hydrogels was obtained when the initial temperature or tube size favored a formation of porous microstructure of hydrogels.

Keywords: initial temperature · microporous materials · polymerization · polymers

Introduction

Frontal polymerization (FP) involves the conversion of a monomer to a polymer through a localized exothermic reaction zone that propagates through the coupling of thermal diffusion and Arrhenius reaction kinetics. The simplest free radical polymerization reactor consists of a test tube filled with a monomer and an initiator. Once the reaction is initiated at the top of the tube by adding heat, the narrow reaction zone, polymerization front, travels down the tube with a constant velocity, creating hot, solid polymer as the reaction progresses. Because reaction becomes self-propagating after an initial input of heat, FP is an energy-saving way of producing polymer materials with the additional advantage of short reaction times.

From its first discovery in Russia,[1] frontal polymerization has been used to prepare different materials, including thermochromic composite,[2] optical gradient materials,[3] temperature-sensitive hydrogels,[4] and simultaneous interpenetrating polymer networks.[5] The application of FP to synthesize copolymers has been investigated.[6–8] Recently, FP was used by Fiori and Mariani for the synthesis of polyurethane,[9] by McFarland and Pojman for the polymerization of 1,6-hexanediol diacrylate with a microencapsulated initiator.[10] In these examples, the rapid reaction rate, observed in propagating fronts, circumvents phase separation which occurs commonly in batch studies. Also, in the case of copolymerization the FP process tends to produce rather narrow chain composition distributions with respect to all other traditional polymerization processes. In addition, because of the high temperature reached by the propagating fronts, polymerization runs can be performed without removing the inhibitor from the monomers.

We have recently demonstrated the feasibility of self-propagating fronts in the synthesis of grafting copolymer hy-

[a] Prof. Dr. Q.-Z. Yan, W.-F. Zhang, G.-D. Lu, Dr. X.-T. Su, Prof. Dr. C.-C. Ge
Laboratory of Special Ceramics and Powder Metallurgy
University of Science and Technology Beijing
Beijing 100083 (China)
Fax: (+86) 010-6233-2472
E-mail: ccge@mater.ustb.edu.cn

drogels.[11] It has been found that this fast and efficient way of producing starch-grafted-acrylic acid hydrogels provides a substantial improvement in terms of conversion, swelling capacity and swelling rate, which are the desired features of hydrogels.

Evidently FP is a very promising technique and one to be widely explored. In all previous works on FP a number of aspects have been explored, such as the effect of initiator type and concentration on front velocity[10,12,13] and the effect of pressure[14] and tube orientation,[15] the dependences of front velocity and front temperature on reaction components.[9,11] In fact FP is performed in a nonadiabatic reactor under the atmosphere in order to test the applicability of this technique to process conditions often found in practice. Thus the environmental conditions such as temperature and reactor size are the key factors for the formation and traveling behavior of self-propagating thermal front[13,16] and the consequent material properties. In all previous works on FP no systematic study on the influence of environmental conditions has been undertaken.

In our previous work, we focused on studying the influence of the relative amounts of reaction components on the front parameters and polymer properties through frontal polymerization synthesis of starch-grafted poly(acrylic acid) hydrogels. In this work we report on the effects of temperature and tube size on the propagating front and properties of hydrogels. We prepared two sets of starch-grafted poly(acrylic acid) hydrogels at various initial temperatures and tube sizes by FP. Ignition time, front velocity and its maximum temperature were the parameters of main interest. The hydrogels were characterized by sol content, gel content and swelling capacity.

Results and Discussion

Frontal polymerization synthesis of graft copolymers: In general, to make a starch-grafted hydrogel by frontal polymerization, the reaction mixture containing appropriate amounts of generalized starch, acrylic acid neutralized partially by a sodium hydroxide solution, initiator ammonium persulfate solution, and crosslinker methylene bisacrylamide solution was poured into a glass tube. The tube was fixed in a chamber drying oven. The graft-polymerization process was initiated by application of a soldering iron to the top of the test tube until the formation of a hot propagating front began. The duration time from the beginning of adding heat to the formation of self-propagating front was defined as ignition time. Front propagation occurred at constant velocity; the position of the front was obvious because of the difference in the optical properties of polymer and initial materials. A plot of the front position versus time produced a straight line; the slope of this line was the front velocity. The temperature profiles were measured by using a K-type thermocouple connected to a digital thermometer.

The inner diameter of tube was varied from 10 to 45 mm for one series of runs and a number of tubes at the same inner diameter (15 mm) for a series in which the oven temperature was varied. The oven temperature was varied from 25 to 60 °C to give a range of initial temperatures for the series of runs and 30 °C for the series in which the tube size was varied. In these two ranges a steady-state polymerization front was observed. Both lower and higher values excluded the existence of steady-state propagation front: at lower values the propagating front was not self-sustainable, whereas at larger values, spontaneous polymerization occurred. The propagating behavior of the polymerization fronts and the corresponding properties of polymers at different reaction conditions are given in Tables 1 and 2.

Ignition time and bubbles: Ignition times ranged from 3.2 to 0.96 min as the initial temperature was raised from 25 to 60 °C as shown in Table 1 and from 1.36 to 35 min as the tube size (i.d.) was raised from 10 to 45 mm as shown in Table 2.

In each case there was an initial period when the reaction mixture was preheated. At the longer ignition times frontal polymerization only became apparent near the end of the

Table 1. Propagating features of the polymerization front and characteristics of hydrogels for different initial temperature.

Run no.	Initial temp. [°C]	Ignition time [min]	Frontal velocity [cm min^{-1}]	Frontal temp. [°C]	Sol [%]	Gel [%]	Equilibrium swelling [g g^{-1}]
1	25	3.2	0.27	98	5.2	96	534
2	30	2.84	0.32	104	7.9	93.5	651
3	35	2.5	0.37	108	10.8	90	783
4	40	2	0.43	112	16.6	88.1	872
5	45	1.67	0.49	117	18.7	85.6	1069
6	50	1.38	0.56	120	19.0	74.7	865
7	55	1.2	0.61	122	19.6	76.3	683
8	60	0.96	0.63	125	18.7	80.4	508

Table 2. Propagating features of the polymerization front and characteristics of hydrogels for different tube size (i.d.).

Run no.	I.d. [mm]	Ignition time [min]	Frontal velocity [cm min^{-1}]	Frontal temp [°C]	Sol [%]	Gel [%]	Equilibrium swelling [g g^{-1}]
1	10	1.36	0.26	95	3.6	97	516
2	15	2.57	0.31	103	7.6	94.1	693
3	20	3.3	0.39	108	8.5	88.7	740
4	25	4.95	0.44	110	9.8	85.8	783
5	30	7	0.47	116	11.4	82	898
6	40	24.2	0.46	113	17	73.6	912
7	45	35	0.44	114	23.2	68.4	907

period. For example, for a tube size of 45 mm nothing appeared to be happening for the first 33 min, and then a vigorous reaction suddenly occurred within seconds, and a propagating front formed within 2 min.

It is well known that an inhibition period exists in the presence of oxygen for free radical polymerizations in general and for acrylic monomers in particular.[17,18] Studies have shown that oxygen essentially forms an alternating copolymer with the monomer, that is, a polyperoxide (-M-O-O-). Addition of monomer to the peroxy radical is much slower than to the normal polymer radical, resulting in the suppression of the normal propagation reaction. In our experiments there was no attempt to exclude oxygen, and there was an inhibition period which became longer as the initial temperature was reduced or the tube size was increased. The inhibition period is brought to an end as a result of the polyperoxide decomposing and yielding initiator radicals. At some point the concentration of initiating radicals might become high enough to enable significant amounts of normal polymerization to occur, resulting in a sudden vigorous polymerization reaction and propagating front.

The propagating front traveled down the tube and resulted in a large amount of vapor bubbles on the front surface adjacent to the polymer product. Part of these bubbles traveled up into polymer matrix and then came out noisily from the tube, which made the final product soft and lightly yellow. This was the case for tube size in the range 30–45 mm. For smaller tube sizes the reaction was much less vigorous, resulting in fewer bubbles and in the final product being a white, opaque rubbery material.

The source of bubbles is water in the reaction mixture. 1 mg of water will result in about 1.7 cm^3 of water vapor at the front temperature of 100 °C and ambient pressure. Bubbles occasionally interfered by making it difficult to initiate a front if a large bubble collected under the front, insulating the reactant and preventing propagation. This trend was more prominent for larger tube size. Nonetheless, flat fronts with constant frontal velocity were obtained.

For temperature series all the reactions proceeded smoothly. The amounts of gas bubbles became more with the higher level of temperature, and all these bubbles were trapped by the viscose reaction mixture. Apparent characteristics of the as synthesized products over all the temperature range were white and opaque.

Front velocity: The variation of front velocity v_{front} with initial temperature and tube size is presented in Tables 1 and 2. The front velocity increased from 0.27 to 0.63 cm min^{-1} for initial temperatures from 25–60 °C as shown in Table 1. An increase of the initial temperature decreases the amount of heat lost to surroundings, resulting in higher frontal velocity.

But for tube size series the front velocity changed nonmonotonically. The value of v_{front} increased from 0.26 to 0.47 cm min^{-1} as the tube size was increased from 10 to 30 mm, and then decreased to 0.44 cm min^{-1} as the tube size was increased to 45 mm (Table 2). The effect of the tube size on the front velocity can be attributed to two factors: the change of surface-to-volume ratio of tube, which affects the rate of heat conduction, and the escape of gas bubbles from open tube, which removes part of heat from the polymerization front. The increase of the tube size decreases the surface-to-volume ratio of the tube and resulted in the decline in heat loss rate. On the other hand, the amounts of escaping bubbles increased with the tube size which, as mentioned above, removed more reaction heat from polymerization front. The interplay of these two opposite effects determines the actual rate of propagating front.

To investigate the front velocity functional dependence on initial temperature, we carried out additional experiments with different tube sizes. Figure 1 shows an Arrhenius plot of front velocity against initial temperature for three different tube diameters (15, 20, and 25 mm). As can be seen, straight lines can be obtained over low initial temperature of 25–50 °C for tube sizes of 15 and 20 mm and 25–40 °C for tube size of 25 mm. The deviation from straight line at higher temperature is probably attributed to the escape of bubbles from reaction system. From the slope of the plot for the linear relationship between $\ln(v_{front})$ and the inverse of temperature (correlation coefficients, $r^2 > 0.98$), the average apparent activation energy was 24 kJ mol^{-1}.

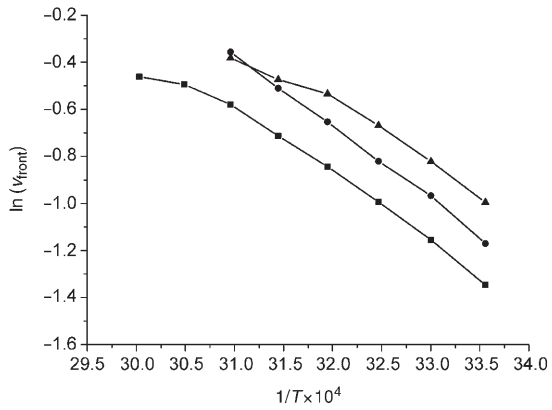

Figure 1. Front velocity dependence on temperature; ■: 15 mm, ●: 20 mm, ▲: 25 mm.

Similarly additional experiments were carried out to investigate the front velocity functional dependence on tube size. Figure 2 shows the dependence of front velocity on the tube size x at three initial temperatures (25, 30, and 35 °C). For three sets the front velocity was found to follow a relationship of higher order with the tube size (linear fitting correlation coefficients, $r^2 > 0.98$), as in Equation (1):

$$v_{front} = (ax^2 + bx + c)^{-1}$$

where a, b, and c are constants related to initial temperature.

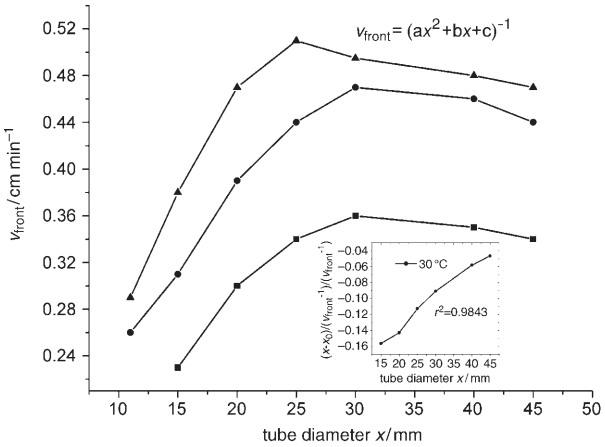

Figure 2. Front velocity dependence on tube size and curve fit at 30 °C (inset) (r: correlation coefficients; x_0, $v_{front\,0}$: a fixed point in v/x curve); ■: 25 °C, ●: 30 °C, ▲: 35 °C.

Front temperature: Temperature gradients in a front are very large, and profile measurements help to elucidate the reasons for incomplete conversion and the structure of the front. Figure 3 shows the temperature profile in a graft copolymerization front of acrylic acid onto starch at different initial temperature. All polymerization fronts had a very sharp temperature profile. This corresponds to a local region completing conversion within a short time.

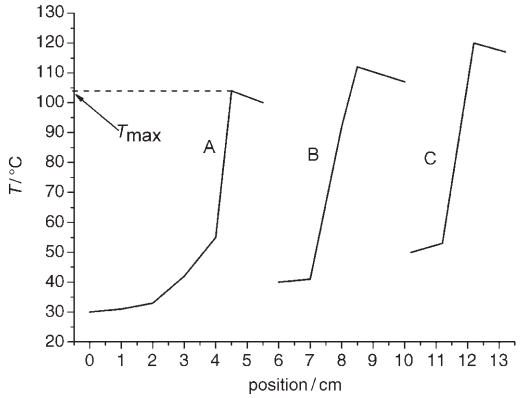

Figure 3. Temperature profiles of acrylic acid grafting onto starch copolymerization fronts at different initial temperatures; A: 30 °C, B: 40 °C, C: 50 °C.

The temperature of the propagating front (T_{max}, as defined in Figure 3) dependence on the experimental conditions was similar to the corresponding v_{front} trend as shown in Tables 1 and 2. Polymerization front is a hot wave, and a high front velocity decreases the time for heat loss, resulting in high front temperature.

Conversion: During the frontal graft copolymerization, some monomers can diffuse to graft onto the starch backbone to form cross-linking networks, which compose the final gel product. Others may be used for the formation of soluble homopolymers and low molecular weight oligomers. The variation of monomer conversion with initial temperature is shown in Table 1. As the temperature was raised from 25 to 60 °C the sol content increased rapidly from 5.2 to 22.5 % and then leveled off at lower value of 19 % as temperature was increased further. The gel content dropped from 96 to 74.7 % as the temperature was raised from 25 to 50 °C and then increased slightly to 80.4 % for temperatures from 50–60 °C.

As mentioned above, increasing the initial temperature increased the front temperature. An increase in the temperature of polymerization front nearly always lowers the molecular weight of the polymer produced regardless of whether the molecular chain length is controlled by chain transfer or by chain termination.[19,20] Thus the amount of the water-soluble oligomers tends to rise with an increase of the initial temperature. But on the other hand, it is well known that the average dimension of the polymer chains approach completely random linking when increasing the temperature to a certain level.[21–24] The active chain ends through hydrogen abstraction can produce new active centers on the polymer backbones. The newly formed free radicals may recombine either with similar radicals or monomers to form random crosslinking networks.[25,26] This random linking of polymer chains tends to reduce sol content and increase gel content.

In the same way the variation of conversion with the tube size is shown in Table 2. The sol content increased from 3.6 to 23.2 % and the gel content dropped from 97 to 68.4 % for the tube diameters from 10 to 45 mm. This is due to the increase in the T_{max} value with tube size, which lowers the molecular weight of the polymer produced.[19,20] In addition, as mentioned above, the amounts of the bubbles escaping from tube increased with increasing tube size. These gas bubbles open the passages for oxygen through the reaction system. The intake of oxygen causes polymer and starch-backbone degradation at high temperature by oxidation.[24] The degradation may proceed by random bond breaking between chain atoms or by peeling off the oligomers from the chain ends, resulting in smaller yellow-colored units.[27] This was supported by the yellow color of other products which became deeper with an increase in tube size. When washing these products, small yellow units dissolved into water and white gels were obtained.

Swelling characteristics: The most salient feature of superabsorbent hydrogels is its high swelling capacity. The swelling capacity showed a maximum of 1069 g g^{-1} at the initial temperature of 45 °C (Table 1). A marked increase in swelling capacity was observed when the initial temperature was raised from 25 to 45 °C, while hydrogels synthesized at higher temperature (50–60 °C) showed a decreasing trend in swelling characteristics.

The swelling of the polymer depends on the fine structure of the polymer network.[28] The rapid temperature increase at the polymerization front and hot front propagating step by step will affect the microstructure of the hydrogels. To confirm this presumption, the microscopic morphologies of

hydrogel samples obtained at initial temperatures of 25, 45, and 55 °C were measured by field emission scanning electron microscope (FE-SEM) (Figure 4). At low initial temperature, less porous structure was observed (Figure 4a). At higher initial temperatures of 45 and 55 °C, irregular porous structures were obtained as illustrated in Figure 4b) and c).

The well-defined pores can be attributed to the high synthesis temperature and rapid temperature increase at the propagating front, which evaporate water to produce gas bubbles. The increase in front temperature with initial temperature results in more bubbles. These bubbles are trapped by sticky reaction mixture and consequently form interconnected capillary channels. High porosity would increase the available space for water during the swollen state.[29] But at higher initial temperature over 45 °C, the effect of the linking mentioned above becomes dominant, resulting in the increase in crosslinking density and decrease in porosity.

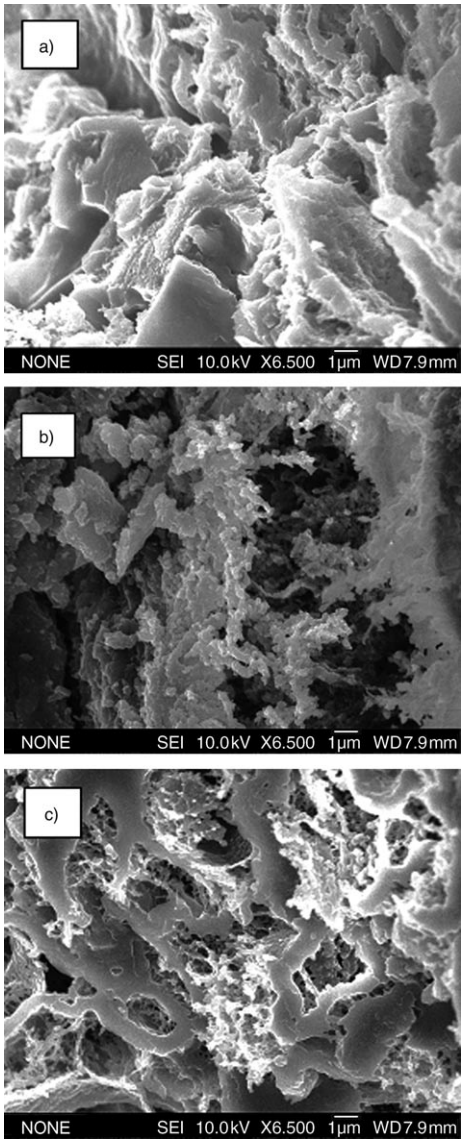

Figure 4. Field emission scanning electron micrographs of hydrogels produced by frontal polymerization at different initial temperatures: a) 25 °C, b) 45 °C, c) 55 °C.

For tube size series we used the amounts of swelling increased from 516 to 898 $g\,g^{-1}$ as the tube size was raised from 10 to 30 mm. For higher tube size values, the swelling capacity remained almost constant at about 900 $g\,g^{-1}$ (Table 2). This is most probably related to the porosity of hydrogels. For tube sizes ranging from 10–30 mm, the number of bubbles increased with tube size, as mentioned above, leading to the increase in porosity of product. But when the tube size was raised to the level higher than 30 mm, some gas bubbles escaped from reaction mixture, only the retaining bubbles were trapped by reaction mixture and formed porous structure. When both the speeds of the bubbles formation and escape from reaction system were enhanced equally with tube size, the porosity of hydrogels would be kept constant. These presumptions were confirmed by FE-SEM images.

Separate swelling experiments were carried out to measure the spatial homogeneity of hydrogels obtained at the center and perimeter of tube for tube sizes of 30 and 45 mm. The deviations were found to be ± 33 and ± 57 $g\,g^{-1}$, respectively, suggesting that hydrogels prepared in these test tubes were spatially uniform.

Conclusion

We studied the effects of the initial temperature and tube size on the propagating front and characteristic properties of starch-grafted poly(acrylic acid) hydrogels. It was observed that an unrestricted access of the reaction mixture to oxygen delayed the formation of the self-propagating polymerization front. The existence of an inhibition period, especially at the large tube size, was attributed to the formation of peroxy radicals with low reactivity. The end of the inhibition period with the onset of rapid, apparently normal polymerization is thought to result from the accumulation of polyperoxide which eventually yields enough active free radicals to overwhelm the inhibition effect of oxygen and set off a self-accelerating process in which the heat released by normal polymerization increases the rates of peroxide and initiator decomposition, and the rise in viscosity restricts the inward flow of oxygen and outward flow of heat. Thus the polymerization front can propagate self-sustainably at constant velocity.

An increase of the initial temperature increased both the front temperature and front velocity, leading to more soluble oligomers, gas bubbles and higher degree of crosslinking. Oligomers raised sol content and reduced gel content. Conversely, crosslinking reduced the sol content and raised the gel content. The interplay of two opposite effects of oligomer and crosslinking determined the sol and gel content. Gas bubbles caused from water evaporation were trapped by the reaction mixture and resulted in the formation of porous copolymers, which was critical for high swelling capacity of hydrogels.

An increase in tube size had two effects on propagating front. One was to raise the front velocity and front temperature due to the reduction in heat loss. The other effect was to reduce the front velocity and front temperature attributed to the increase in the number of escaping gas bubbles. The combined action of two effects resulted in both the front velocity and front temperature exhibiting the maximum values with varying tube sizes. On the other hand, the bubbles which escaped from test tube opened passages for oxygen through the reaction system. The intake of oxygen from air broke polymer molecules already formed into smaller units by the action of oxidation, resulting in the increase in sol content and the reduction in gel content with tube size. The highest degree of swelling for products was obtained when the tube size favor a formation of porous microstructure of hydrogels.

Experimental Section

Materials: The materials used in this study were potato starch containing 5.3 wt % moisture, acrylic acid as the monomer, methylene bisacrylamide as a crosslinker agent, ammonium persulfate as an initiator, and sodium hydroxide. All materials were used as received from Beijing Chemical Company (Beijing, China).

Frontal polymerization: Potato starch (2.5 g) and distilled water (12 g) were mixed and then heated at around 60 °C to form gelatinized starch slurry. Acrylic acid (11 g in 4 g water) was partially neutralized with solution of sodium hydroxide (2 g) in water (5 g). A solution of ammonium persulfate (0.1 g) and methylene bisacrylamide (0.0015 g) in water (2 g) was prepared. Then the monomer solution, the initiator and cross-linking agent solution were added to the gelatinized starch. The mixture was stirred magnetically at room temperature for 30 min.

The reaction mixture was poured into a 200 mm long test tube (i.d. 10–45 mm) to give a range of tube sizes for one series of runs and a number of test tubes at the same inner diameter (15 mm) for a series in which the temperature was varied. A K-type thermocouple, connected to a digital thermometer, was utilized to monitor the temperature change. The junction was immersed at about 6 cm from the free surface of the mixture. The front position and temperature was recorded as a function of time. A plot of the front position versus time produces a straight line; its slope was the front velocity. A temperature profile of the front was obtained by converting the temporal profile to a spatial one using the front velocity. The tube was clamped to a ring stand in a chamber drying oven at a temperature which was in the range 25–60 °C for the series of runs in which the temperature was varied and 30 °C for the series in which the test tube size was varied. The upper layer of the mixture was then heated by soldering iron until the formation of a hot propagating front began. The ignition time was defined as the duration time from the beginning of adding heat to the formation of self-propagating front.

Determination of sol and gel content: After the reaction was completed, the tube was removed from oven and allowed to cool to room temperature. The reaction product was removed and cut into small pieces (2–5 mm) which were immersed in a large excess of sodium chloride solution (1 % wt/wt) and shaken at intervals over a 72 h period to dissolve water-soluble materials. The presence of the salt restricted the amount of swelling and improved the accuracy. Then the mixture was filtered. The gel product was dewatered with methanol and dried in a vacuum oven at 65 °C until the weight of the specimen was constant. The dried polymer product was weighted. The total amount of polymer obtained from the weight of partially neutralized monomer and starch charged was calculated to yield the percentage gel content. The filtrate with known weight of sodium chloride was heated in an air-circulating oven at 90 °C to dryness, and weighted to give the total amount of sol content.

Swelling measurements: Water absorption measurements were performed by filtration method. For dried gel polymers, a fixed amount (0.2 g $\pm$ 0.001) of classified (160–180 μm) product was dispersed in distilled water (500 mL) for 30 min. The swollen samples were filtered through a 200-mesh wire gauze until they no longer slipped from the gauze when it was held vertically. The degree of absorption was determined from the weight gain on the gauze after immersion in water per unit weight of gel before immersion. To obtain a reliable value for absorbing, three values were averaged.

Scanning electronic microscope measurements: Structures of hydrogels obtained were examined using a JEOL field emission scanning electronic microscope (FE-SEM). The samples used for FE-SEM measurement were immersed in distilled water after synthesis to swell to maximum swelling, dehydrated in ethanol and then air dried at 60 °C. Dried samples were cut to expose their inner structure, coated with a layer of carbon.

Acknowledgements

The authors gratefully acknowledge the National Natural Science Foundation of China for financial support (No. 50372008).

[1] N. M. Chechilo, R. J. Khvikivitskii, N. S. Enikolopyan, *Dokl. Akad. Nauk SSSR* **1972**, *204*, 1180–1181.
[2] I. P. Nagy, L. Sike, J. A. Pojman, *J. Am. Chem. Soc.* **1995**, *117*, 3611–3612.
[3] J. Masere, L. L. Lewis, J. A. Pojman, *J. Appl. Polym. Sci.* **2001**, *80*, 686–691.
[4] R. P. Washington, O. Steinbock, *J. Am. Chem. Soc.* **2001**, *123*, 7933–7934.
[5] J. A. Pojman, W. Elcan, A. M. Khan, L. Mathias, *J. Polym. Sci. Part A Polym. Chem.* **1997**, *35*, 227–230.
[6] A. Tredici, R. Pecchini, M. J. Morbidelli, *J. Polym. Sci. Part A Polym. Chem.* **1998**, *36*, 1117–11261.
[7] M. F. Perry, V. A. Volpert, L. L. Lewis, H. A. Nichols, J. A. Pojman, *Macromol. Theory Simul.* **2003**, *12*, 276–286.
[8] N. S. Pujari, A. R. Vishwakarma, T. S. Pathak, S. A. Mule, S. Ponrathnam, *Polym. Int.* **2004**, *53*, 2045–2050.
[9] S. Fiori, A. Mariani, L. Ricco, S. Russo, *Macromolecules* **2003**, *36*, 2674–2679.
[10] B. McFarland, S. Popwell, J. A. Pojman, *Macromolecules* **2004**, *37*, 6670–6672.
[11] Q. Z. Yan, W. F. Zhang, G. D. Lu, X. T. Su, C. C. Ge, *Chem. Eur. J.* **2005**, *11*, 6609–6615.
[12] N. M. Chechilo, N. S. Enilolopyan, *Dokl. Phys. Chem.* **1975**, *221*, 392–394.
[13] J. A. Pojman, J. Willis, D. Fortenberry, V. Ilyashenko, A. M. Khan, *J. Polym. Sci. Part A Polym. Chem.* **1995**, *33*, 643–652.
[14] N. M. Chechilo, N. S. Enilolopyan, *Dokl. Phys. Chem.* **1976**, *230*, 840–843.
[15] M. Bazile Jr. , H. A. Nichols, J. A. Pojman, V. Volpert, *J. Polym. Sci. Part A Polym. Chem.* **2002**, *40*, 3504–3508.
[16] J. A. Pojman, W. W. West, J. Simmons, *J. Chem. Educ.* **1997**, *74*, 727–730.
[17] H. Omidian, S. A. Hashemi, P. G. Saammes, I. G. Meldrum, *Polymer* **1998**, *39*, 3459–3466.
[18] P. J. Flory, *Principles of polymer chemistry*, Cornell University Press, Ithaca and London, **1953**, pp. 168–174.
[19] D. I. Fortenberry, J. A. Pojman, *J. Polym. Sci. Part A Polym. Chem.* **2000**, *38*, 1129–1135.
[20] P. J. Flory, *Principles of polymer chemistry*, Cornell University Press, Ithaca and London, **1953**, pp. 145–146.
[21] M. L. Huggins, *Physical chemistry of high polymer*, Wiley, New York, **1958**, pp. 35–36.
[22] G. F. Fanta, E. B. Bagley, R. C. Burr, W. M. Doane, *Starch/Staerke* **1982**, *34*, 95–102.

[23] M. L. Huggins, *Physical chemistry of high polymer*, Wiley, New York, **1958**, pp. 14.
[24] S. Kiatkamjornwong, P. Phunchareon, *J. Appl. Polym. Sci.* **1999**, *72*, 1349–1366.
[25] R. Poli, F. Stoffelbach, S. Maria, J. Mata, *Chem. Eur. J.* **2005**, *11*, 2537–2548.
[26] C. Wetter, J. Gierlich, C. A. Knoop, C. Müller, T. Schulte, A. Studer, *Chem. Eur. J.* **2004**, *10*, 1156–1166.
[27] D. R. Patil, G. F. Fanta, *J. Appl. Polym. Sci.* **1993**, *47*, 1765–1772.
[28] P. J. Flory, *Principles of polymer chemistry*, Cornell University Press, Ithaca and London, **1953**, pp. 576–593.
[29] X. Z. Zhang, D. Q. Wu, C. C. Chu, *Biomaterials* **2004**, *25*, 3793–3805.

Received: August 9, 2005
Published online: February 7, 2006

